CT53518, a novel selective FLT3 antagonist for the treatment of acute myelogenous leukemia (AML)

Louise M. Kelly,[1,2,7] Jin-Chen Yu,[5,7] Christina L. Boulton,[1] Mutiah Apatira,[5] Jason Li,[5] Carol M. Sullivan,[5] Ifor Williams,[3] Sonia M. Amaral,[1,2] David P. Curley,[1] Nicole Duclos,[1,2] Donna Neuberg,[4] Robert M. Scarborough,[5] Anjali Pandey,[5] Stanley Hollenbach,[5] Keith Abe,[5] Nathalie A. Lokker,[5] D. Gary Gilliland,[1,2,6] and Neill A. Giese[5,6]

[1]Division of Hematology/Oncology, Brigham and Women's Hospital, Boston, Massachusetts 02115
[2]Howard Hughes Medical Institute, Harvard Medical School, Boston, Massachusetts 02115
[3]Department of Pathology, Emory University, Atlanta, Georgia 30322
[4]Dana-Farber Cancer Institute, Boston, Massachusetts 02115
[5]Millennium Pharmaceuticals, Inc., 256 E. Grand Avenue, South San Francisco, California 94080
[6]Correspondence: gilliland@calvin.bwh.harvard.edu (D.G.G.), neill.giese@mpi.com (N.A.G.)
[7]These authors contributed equally to this work.

Summary

Up to 30% of acute myelogenous leukemia (AML) patients harbor an activating internal tandem duplication (ITD) within the juxtamembrane domain of the FLT3 receptor, suggesting that it may be a target for kinase inhibitor therapy. For this purpose we have developed CT53518, a potent antagonist that inhibits FLT3, platelet-derived growth factor receptor (PDGFR), and c-Kit (IC_{50} ~200 nM), while other tyrosine or serine/threonine kinases were not significantly inhibited. In Ba/F3 cells expressing different FLT3-ITD mutants, CT53518 inhibited IL-3-independent cell growth and FLT3-ITD autophosphorylation with an IC_{50} of 10–100 nM. In human FLT3-ITD-positive AML cell lines, CT53518 induced apoptosis and inhibited FLT3-ITD phosphorylation, cellular proliferation, and signaling through the MAP kinase and PI3 kinase pathways. Therapeutic efficacy of CT53518 was demonstrated both in a nude mouse model and in a murine bone marrow transplant model of FLT3-ITD-induced disease.

Introduction

Acute myelogenous leukemia (AML) is a clonal hematopoietic stem cell disorder that increases in incidence with age and represents ~90% of all acute leukemias in adults (Lowenberg et al., 1999). Although induction chemotherapy results in complete remission in 50%–75% percent of patients, relapse is common and long-term survival rates remain at <20%. Thus, more effective treatment strategies are needed. Targeted inhibition of aberrant kinase signaling can be an effective therapeutic intervention in hematologic malignancies, as evidenced by hematologic and cytogenetic responses in chronic myelogenous leukemia (CML) and CML blast crisis patients treated with the BCR/ABL kinase inhibitor STI571 (Carroll et al., 1997; Druker and Lydon, 2000; Druker et al., 2001a, 2001b; Savage and Antman, 2002). An analogous kinase inhibitor strategy may be useful in AML patients with activating mutations in FLT3. The most common FLT3 mutation, found in up to 30% of patients, is an internal tandem duplication (ITD) within the juxtamembrane domain, and an additional 7% have a point mutation in the kinase activation loop (Abu-Duhier et al., 2001; Kiyoi et al., 1999; Kottaridis et al., 2001; Nakao et al., 1996; Rombouts et al., 2000; Whitman et al., 2001; Yamamoto et al., 2001; Yokota et al., 1997). FLT3 is an attractive target for therapeutic intervention as the single most commonly mutated gene in AML and because FLT3 mutations confer a poor prognosis (Abu-Duhier et al., 2000; Kiyoi et al., 1999; Kottaridis et al., 2001; Stirewalt et al., 2001). We have developed CT53518, a potent FLT3 antagonist of the piperazinyl quinazoline class that also inhibited PDGFR and c-Kit but did not have significant activity against a wide range of other kinases. CT53518 is a potent inhibitor of FLT3-ITD-transformed hematopoietic cell lines and of human AML cell lines expressing the mutant FLT3 receptor. In addition, CT53518 is a potent inhibitor in murine models of FLT3-ITD-mediated disease. Taken together, these data indicate that, by analogy with activity of STI571 in CML blast crisis, CT53518

SIGNIFICANCE

Most adults who develop AML die from their disease or complications of cytotoxic chemotherapy. Constitutively activated FLT3 (FLT3-ITD) represents the single most common mutation in AML and confers a poor prognosis. FLT3-ITD is thus an attractive potential therapeutic target for tyrosine kinase inhibition. We have developed CT53518, which selectively blocks FLT3-ITD phosphorylation, leading to an inhibition of Erk2 and Akt signaling and to induction of apoptosis in FLT3-ITD-positive human AML cell lines. In animals, CT53518 is orally bioavailable, has suitable pharmacokinetic and toxicity profiles for clinical use, and is efficacious in murine models of FLT3-ITD-mediated disease. CT53518 may be a useful therapeutic agent in the treatment of FLT3-ITD-positive AML and is currently under evaluation in clinical trials.

Table 1. Specificity and potency of CT53518 kinase inhibitor

	CT53518	Staurosporin
Receptor tyrosine kinases	IC_{50}	IC_{50}
βPDGFR	0.20 μM	0.08 μM
FLT3	0.22	0.10
c-Kit	0.17	0.01
CSF-1R	3.43	0.12
KDR	>30	0.02
EGFR	>30	ND
FGFR	>30	0.42
InsR	>30	<0.3
Nonreceptor tyrosine kinases		
Src	30	0.07
Abl	>30	0.10
Ser/Thr kinases		
PKC, PKA	>30	0.08
MAP kinases and MAPK kinases		
Mek1, Mkk4, Mkk6, Erk2, p38	>30	<1

Autophosphorylation of all receptor tyrosine kinases were measured in intact cells using a two-site enzyme-linked immunosorbent assay except for InsR which, together with the cytoplasmic receptors, was assayed using purified enzyme. See Experimental Procedures.

may have therapeutic value in AML associated with activating mutations in FLT3.

Results

Selective kinase inhibition by CT53518

Novel small molecule FLT3 kinase inhibitors of the piperazinyl quinazoline class were identified by screening of chemical libraries. The specificity of an optimized analog, CT53518, was then tested against a wide range of kinases. The relative kinase inhibitory activity of CT53518 was first tested in the related type III RTKs as previously described (Yu et al., 2001). CT53518 inhibited FLT3, PDGFR, and c-Kit with an IC_{50} of 170–220 nM in in vitro kinase assays, whereas 15- to 20-fold higher concentration was required to inhibit CSF-1R (Table 1). When similar cell-based assays for the FGFR, EGFR, and KDR receptor tyrosine kinases or purified enzyme assays for insulin receptor, cytoplasmic tyrosine kinases, serine/threonine kinases, or members of the MAPK cascades were performed, no significant inhibition was observed at >100-fold higher concentrations (Table 1). In control experiments, staurosporin inhibited all kinases with an IC_{50} of <1 μM (Table 1). These studies demonstrated that CT53518 is a potent and highly selective inhibitor of FLT3, c-Kit, and PDGFR. Inhibition was reversible since PDGF-induced autophosphorylation rapidly returned to pretreatment level following withdrawal of CT53518 (data not shown).

CT53518 inhibits FLT3-ITD autophosphorylation and mitogenic signaling in Ba/F3 cells

We next tested the ability of CT53518 to inhibit constitutively activated FLT3-ITD mutants cloned from AML patients (W51, W73, W78, Npos, and T6) (Kelly et al., 2002). Stable expression of each of these five cDNAs confers IL-3-independent growth

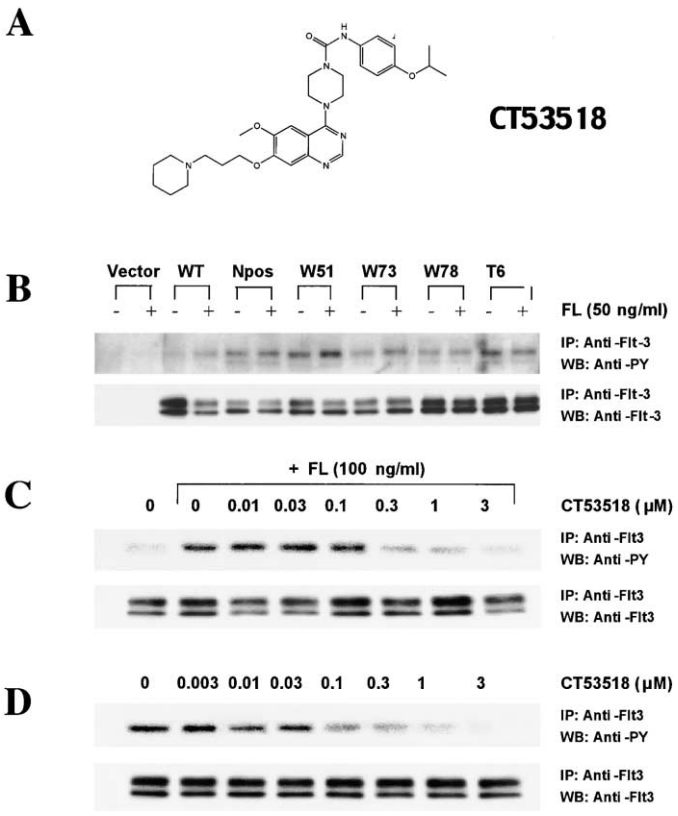

Figure 1. Effect of CT53518 on ligand-stimulated and constitutive phosphorylation of FLT3

A: Chemical structure of CT53518. The chemical name is 4-[6-methoxy-7-(3-piperidine-1-yl-propoxy)-quinazolin-4-yl]-piperazine-1-carboxylic acid (4-isopropoxyphenyl) amide (MF = $C_{31}H_{42}N_6O_4$, MW = 562.7).

B: Constitutive phosphorylation of FLT3-ITD mutants in Ba/F3 cells. Ba/F3 cells expressing wild-type FLT3 (wt) or each of the five FLT3-ITD mutants (Npos, W51, W73, W78, and T6) were unstimulated (−) or stimulated (+) with 50 ng/ml of recombinant human FLT3 ligand (FL). Cell lysates were prepared and FLT3 protein was immunoprecipitated with anti-FLT3 polyclonal antibody, resolved by SDS-PAGE, and immunoblotted with either anti-phosphotyrosine monoclonal antibody or anti-FLT3 polyclonal antibody, as indicated.

C and D: CT53518 inhibits phosphorylation of wt FLT3 and FLT3-ITD in Ba/F3 cells. Ba/F3 cells expressing wt FLT3 (**C**) and W51 FLT3-ITD (**D**) were incubated with the indicated concentrations of CT53518, and cells expressing wt FLT3 were then unstimulated (−) or stimulated (+) with 100 ng/ml of FL. Cell lysates were prepared and FLT3 protein was immunoprecipitated followed by immunoblot analysis using either anti-phosphotyrosine monoclonal antibody or anti-FLT3 polyclonal antibody as shown.

to Ba/F3 cells, allowing the system to be used to study FLT3-ITD-specific signaling. The level of receptor tyrosine phosphorylation was measured in the absence or presence of 50 ng/ml FLT3 ligand (FL) (Figure 1B). FLT3 was immunoprecipitated from cell lysates, proteins were separated by SDS-PAGE, and immunoblot analyses were performed using anti-phosphotyrosine monoclonal antibody PY99 or anti-FLT3 polyclonal antibody. All five FLT3-ITDs exhibited a high level of autophosphorylation with little augmentation by addition of FL, whereas autophosphorylation of wild-type FLT3 was only observed upon ligand stimulation (Figure 1B). To examine the inhibitory activity of CT53518 against FLT3-ITDs, Ba/F3 cells expressing the W51 mutant were incubated with various concentrations of CT53518 (0.003–3 μM)

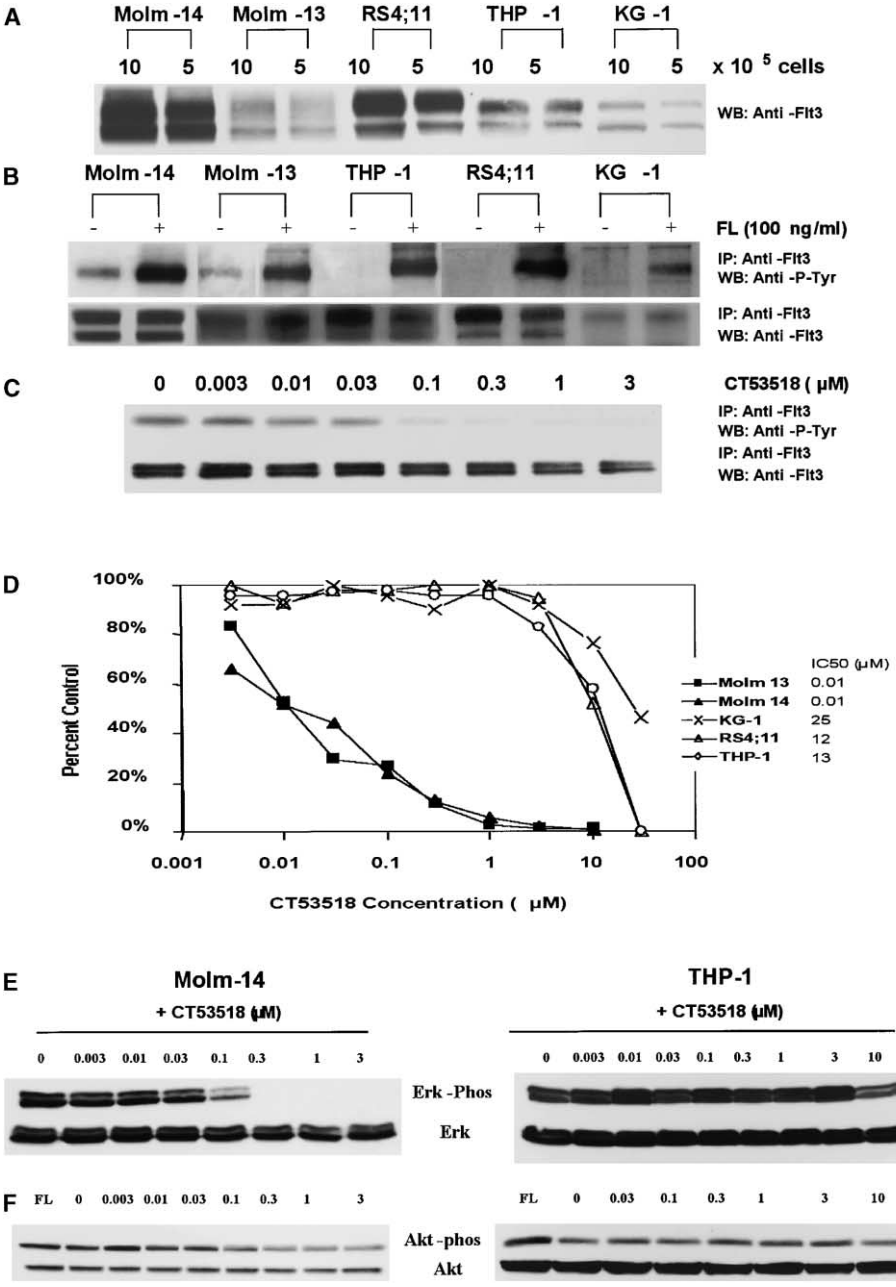

Figure 2. CT53518 inhibits FLT3-ITD-induced proliferation and intracellular signaling in AML cell lines

A: FLT3 receptor levels in leukemia cell lines. Cell lysates from 5×10^5 or 10×10^5 cells of leukemia cell lines Molm-14, Molm-13, RS4;11, THP-1, and KG-1 were prepared, subjected to SDS-PAGE analysis, and immunoblotted with anti-FLT3 polyclonal antibody. Shown is a representative blot of three separate experiments.

B: FLT3 tyrosine phosphorylation in leukemia cell lines. Molm-14, Molm-13, RS4;11, THP-1, and KG-1 leukemia cells were either unstimulated (−) or stimulated (+) with 100 ng/ml of FL and cell lysates were prepared. FLT3 protein was immunoprecipitated followed by immunoblot analysis using an anti-phosphotyrosine monoclonal antibody.

C: Effect of CT53518 on tyrosine phosphorylation of FLT3-ITD in Molm-14 AML cells. Molm-14 cells were incubated with indicated concentrations of CT53518 and cell lysates were prepared. FLT3 protein was immunoprecipitated followed by immunoblot analysis using anti-phosphotyrosine monoclonal antibody or anti-FLT3 polyclonal antibody as indicated.

D: CT53518 inhibits proliferation of AML cells expressing FLT3-ITD. We plated 3×10^4 of the indicated leukemia cells in 1 ml of culture media in the presence of increasing concentrations of CT53518 (0.004–30 μM). Cells were grown for 3 days in tissue culture and viable cells were counted. Shown are representative growth curves of three independent experiments.

E and F: CT53518 inhibits Erk and Akt phosphorylation in FLT3-ITD-positive AML cells. Molm-14 and THP-1 AML cells were incubated with indicated concentrations of CT53518. Cell lysates were prepared and resolved on SDS-PAGE followed by immunoblot analysis using anti-phospho-Erk2 or anti-phospho-Akt1 as well as anti-Erk and anti-Akt antibodies as indicated. FL-stimulated control sample shown in **F**.

prior to cell lysis. As a comparison, the same experiments were performed with cells expressing wild-type FLT3 that were stimulated with FL. CT53518 inhibited wild-type FLT3 or W51 tyrosine phosphorylation with an IC_{50} of 30–100 nM (Figures 1C and 1D). Similar results were obtained with Ba/F3 cells expressing Npos and T6 FLT3-ITDs (data not shown).

To determine the effect of CT53518 on FLT3-ITD-mediated cell growth, Ba/F3 cells expressing each mutant were grown in increasing concentrations of inhibitor and viable cells were counted 3 days later. In the absence of CT53518, the number of cells increased 5- to 10-fold, and this growth was inhibited by CT53518 with IC_{50} values of 10–30 nM (Table 2). Inhibition was specific for FLT3-ITD-mediated cell growth since the growth inhibition could be rescued with IL-3, and ~1000-fold higher concentrations of CT53518 were required to cause nonspecific toxicity (data not shown). CT53518 inhibition of proliferation was also evaluated in Ba/F3 cells transformed to IL-3-independent growth by TEL/PDGFβR, TEL/TRKC, or BCR/ABL, respectively. CT53518 effectively inhibited growth of TEL/PDGFβR transformed cells at 30 nM when compared to untreated cells or cells transformed with BCR/ABL or TEL/TRKc (Table 2). These data further confirm the inhibition of the type III RTKs (including PDGFβR, KIT, and c-FMS) by CT53518 and the lack of inhibition of other tyrosine kinases including ABL and TRKc. This result also indicates that nonspecific cytotoxic effects are not observed within the effective range of drug concentration. It should be noted that the IC_{50} values for growth inhibition were approximately 20- to 50-fold lower in Ba/F3 cells

Table 2. CT53518 inhibits FLT3/ITD-mediated Ba/F3 cell proliferation

Cell Line	IC_{50} (μM)
WT	ND
T6	0.01
Npos	0.02
W73	0.03
W78	0.02
W51	0.02
TEL/PDGFR	0.02
TEL/TRKC	2.00
BCR/ABL	25.0

Cells (3×10^4) were grown in medium without IL-3 and in the presence of increasing concentrations of CT53518 (0.004–30 μM). Viable cells were counted after 3 days and the concentration of CT53518 that inhibits 50% growth was determined. Shown are representative data from three independent experiments.

than the level required for FLT3 enzyme inhibition in CHO cells (Figure 1D) and may reflect the low levels of FLT3 expression in Ba/F3 cells.

Role of FLT3-ITD signaling in human leukemia cells

To extend these studies to a more clinically relevant system, the effect of CT53518 inhibition of FLT3 on the growth and survival of human leukemia cell lines was examined. FLT3 RNA was detected in the leukemia cell lines KG-1, RS4;11, THP-1, Molm-13, and Molm-14 cells (Matsuo et al., 1997; Yokota et al., 1997) using Taqman analysis (data not shown). By Western blot analysis, Molm-14 and RS4;11 had the highest level of FLT3 expression. THP-1 had an intermediate level, whereas 10- to 20-fold less FLT3 expression was observed in Molm-13 and KG-1 (Figure 2A). Quantitative measurement of FLT3 protein estimated a range of 1,000–10,000 receptors per cell (data not shown). Previous screening of leukemia cell lines for FLT3-ITD mutations identified a 7 codon ITD in Molm-13, but the effect of this mutation on receptor phosphorylation and signaling was not determined (Yokota et al., 1997). Sequence analysis revealed that the FLT3-ITD in Molm-13 and Molm-14 contained an additional phe codon at the 5′ end of a 6 codon ITD (DFREYE, amino acids 593–598) (data not shown). Both Molm cells also expressed wild-type FLT3, while there were no FLT3-ITD mutations found in THP-1, KG-1, or RS4;11. To evaluate the level of FLT3 activation in these leukemia cell lines, FLT3 autophosphorylation was measured using anti-phosphotyrosine Western blot analysis. Ligand-independent FLT3 phosphorylation was observed in Molm-13 and Molm-14, whereas FLT3 phosphorylation in THP-1, KG-1, and RS4;11 cells was only seen following FL stimulation (Figure 2B). There was, however, significant stimulation of autophosphorylation by FL in the Molm-13 and Molm-14 cells lines, which may be due to further stimulation of the FLT3-ITD allele, or stimulation of wild-type FLT3 receptor in these cells. More importantly, pretreatment of Molm 14 with CT53518 inhibited the constitutive FLT3-ITD phosphorylation with an IC_{50} of ~30 nM (Figure 2C). These studies demonstrate that the endogenous FLT3-ITD expressed in Molm cells is activated but can be selectively inhibited by CT53518.

STI571 treatment of myeloid or lymphoid cells that express BCR/ABL blocks proliferation and induces apoptosis, whereas Philadelphia chromosome (Ph)-negative leukemia cells are unaffected (Beran et al., 1998; Druker et al., 1996; Fang et al., 2000; Oetzel et al., 2000). To explore the possibility that FLT3-ITD signaling plays a similar role in AML cells, Molm, THP-1, KG-1, and RS4;11 cells were incubated with increasing concentrations of CT53518 (0.004–30 μM) and cell growth was monitored. CT53518 inhibited cell proliferation of the FLT3-ITD-positive Molm-13 and Molm-14 with an IC_{50} of 10 nM, whereas the FLT3-ITD-negative THP-1, KG-1, and RS4;11 cells were highly resistant, requiring 1000-fold higher concentrations to inhibit cell growth (Figure 2D).

For the other type III RTK family members, the MAP kinase, PI-3 kinase, Src kinase, and STAT pathways play an important role in oncogenic transformation, but the role of these pathways in FLT3-ITD signaling in AML cells is less well characterized (Birkenkamp et al., 2001; Iida et al., 1999; Towatari et al., 1997). Since FLT3-ITD signaling is required for Molm-14 AML cell growth and survival, selective inhibition by CT53518 was utilized to investigate the role of the MAP and PI-3 kinase pathways. As a measurement of MAP kinase signaling, the level of Erk2 phosphorylation was determined by Western blot analysis of Molm-14 cells following incubation with increasing concentrations of CT53518 (0.003–3 μM). A high level of constitutive Erk2 phosphorylation was observed in Molm-14 cells that could be completely inhibited by 300 nM CT53518 (Figure 2E). Similarly, high levels of phospho-Erk2 were detected in THP-1 cells, but treatment with CT53518 at concentrations up to 3 μM had little or no effect on Erk2 phosphorylation (Figure 2E). RTKs commonly utilize the PI-3 kinase pathway to promote cell survival through recruitment of Akt to the plasma membrane, resulting in its activation by phosphorylation (Blume-Jensen and Hunter, 2001; Stephens et al., 1998; Stokoe et al., 1997). Therefore, anti-phospho-Akt Western blot analysis was performed on Molm-14 cells to assess the level of Akt phosphorylation as a measurement of PI-3 kinase pathway activation. As with Erk2, a constitutively high level of Akt phosphorylation was readily detected and was efficiently blocked by pretreatment of the Molm-14 cells with 100–300 nM CT53518 (Figure 2F). THP-1 cells also showed constitutive Akt phosphorylation, but this was unaffected by treatment with CT53518 at concentrations up to 10 μM.

To determine if inhibition of Molm cell proliferation was accompanied by apoptosis, annexin-V binding was monitored by flow cytometry. Treatment of FLT3-ITD-positive Molm-14 cells with CT53518 resulted in an increase in the percentage of annexin-V binding cells from a background level of 5% to 51% at 24 hr and 78% at 96 hr (Figure 3). As expected, CT53518 treatment of FLT3-ITD-negative THP-1 cells had no effect on annexin-V binding. To further demonstrate that the induction of apoptosis by CT53518 was due to FLT3 inhibition, treatment of Molm-14 cells with STI571, which inhibits c-Kit and PDGFβR but not FLT3, had no affect on annexin-V binding (Figure 3). These results established that FLT3-ITD-activated cellular signaling pathways are essential for these AML cell lines proliferation and survival.

Evaluation of CT53518 in vivo in a nude mouse model

We first tested the efficacy of CT53518 in a murine model in which FLT3-ITD-transformed Ba/F3 cells were injected into nude mice resulting in tumor development and death. As noted above, FLT3-ITD cDNAs cloned from patient AML samples were expressed in IL-3-dependent Ba/F3 cells. Although these cells no longer require IL-3 for growth, their proliferation and survival

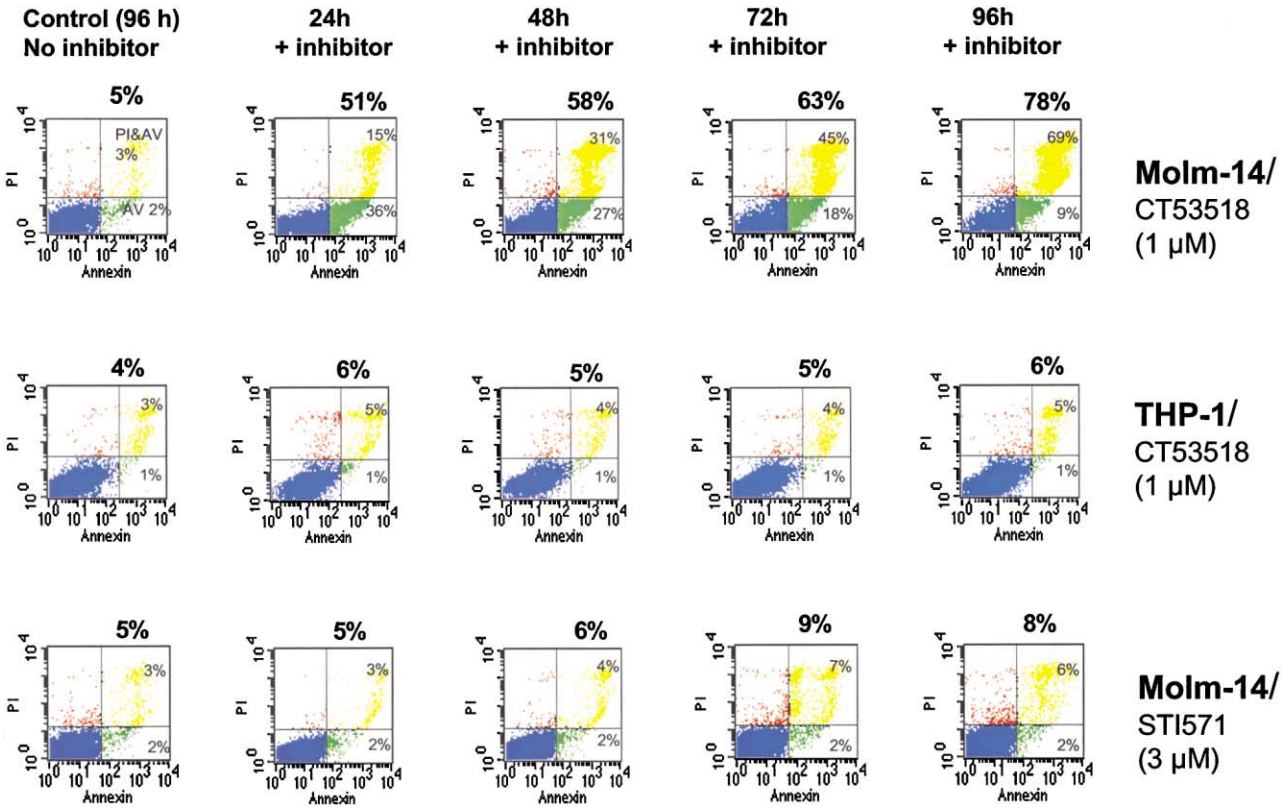

Figure 3. CT53518 induces apoptosis in FLT3-ITD-positive AML cells

Molm-14 and THP-1 AML cells were cultured in growth medium in the presence of 1 μM CT53518 or 3 μM STI571. Cells were harvested daily and stained with annexin V-FITC and propidium iodide followed by flow cytometric analysis. Total percentage of annexin V-positive cells is shown on top of each diagram. Shown are representative data from three independent experiments.

was dependent on FLT3-ITD signaling that was inhibited by CT53518 with an IC_{50} of 10–30 nM (Table 2). To evaluate the in vivo efficacy of CT53518, 20 female athymic nude (nu/nu) mice were injected via tail vein with 1×10^6 W51 cells, and the animals were divided into treatment and vehicle control groups ($n = 10$/group). Starting on day 7 postinoculum, CT53518 was administered by oral gavage at 60 mg/kg bid until day 42, whereas the control group received the 0.5% methylcellulose vehicle only. Mortality of 100% was observed by day 40 for the vehicle control group, whereas CT53518 treatment caused a statistically significant ($p < 0.001$ by a log rank test) increase in survival that was extended on average by 20 days (Figure 4A). In a second study, animals were dosed under the same protocol at either 60 mg/kg bid or 20 mg/kg bid. When compared to vehicle controls, a significant ($p < 0.05$) increase in survival was observed at both doses with a 10% or 20% cure rate at the low and high doses, respectively (Figure 4B). Monitoring of CT53518 levels determined that the average nadir plasma concentration (66 nM) may not have been sufficient to completely block FLT3 throughout the dosing period and suggest that optimal responses may require higher dose levels in this murine model (data not shown).

In vivo efficacy of CT53518 in a bone marrow transplant model of FLT3-ITD-induced myeloproliferative disease

We next tested in vivo efficacy of CT53518 in primary hematopoietic cells transformed by FLT3-ITD. Trials were performed using a murine bone marrow transplant (BMT) assay for FLT3-ITD-induced myeloproliferative disease (Kelly et al., 2002). To best mirror a human treatment regimen, we chose to assess efficacy of CT53518 in established disease. Our previous observations with the FLT3-ITD BMT assay indicated that disease was well established at approximately 30 days posttransplant and that >90% of animals succumbed to disease by day 60 (Kelly et al., 2002). Moribund mice with splenomegaly were sacrificed during the trial and all remaining mice were sacrificed at trial endpoint. Three independent trials were performed and involved a total of 35 placebo and 33 drug-treated animals. In trial 1, mice were treated with drug from day 32; in trials 2 and 3, drug was administered from day 25.

Characterization of the pharmacokinetic properties of CT53518 in Balb/c mice

Pharmacokinetic properties of CT53518 were evaluated in 27 Balb/c mice dosed by oral gavage at 60 mg/kg, and serial plasma samples were collected for determination of compound concentrations. Following gavage, a peak plasma concentration of 3.3 μM was observed at 1 hr and the estimated terminal phase half-life was 2.87 hr (Figure 5E). At 10 hr after dosing, plasma concentrations were 200 nM approaching the IC_{90} of 300 nM, indicating that adequate drug coverage could be achieved with bid dosing. On the last day of trial 2, 2–3 animals each in the drug-treated group were sacrificed at 2, 6, and 12 hr post morning dose, and their plasma samples were taken to

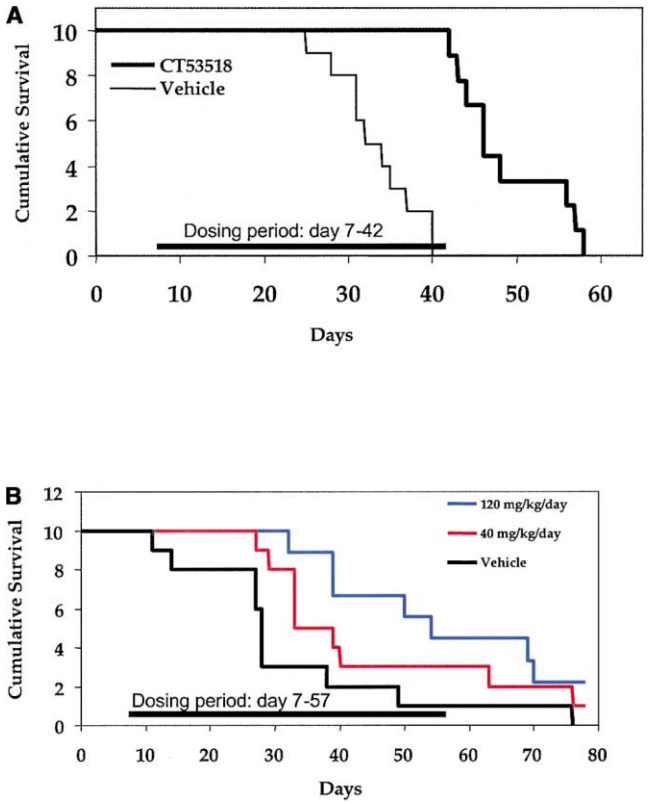

Figure 4. CT53518 treatment increases survival in a Ba/F3 nude mouse model of FLT3-ITD-mediated leukemia

Nude mice (n = 10 for each CT53518-treated or vehicle control group) were each injected via tail vein with 1×10^6 Ba/F3 cells expressing W51 FLT3-ITD mutant. BID dosing via oral gavage was started on 7 days post cell injection in two separate studies with either vehicle or 60 mg/kg of CT53518 suspended in 0.5% methyl cellulose (**A**) or with either vehicle, 20 or 60 mg/kg of CT53518 (**B**). Dosing was terminated on 42 or 57 days post cell injection as indicated.

measure CT53518 concentration. The average plasma concentration of CT53518 was 766 nM (431 ng/ml) at 2 hr, 361 nM (203 ng/ml) at 6 hr, and 266 nM (150 ng/ml) at 12 hr (Figure 5F). In general, these steady-state concentrations were consistent with those obtained in the single-dose PK analysis and were above the IC_{50} of CT53518 for FLT3. More detailed pharmacokinetic studies were performed in dog and monkey in which oral bioavailability ranged from 50%–100% and the terminal plasma half-life was 7–16 hr (data not shown).

Outcome of CT53518 trials in the murine FLT3-ITD BMT model

Kaplan-Meier analyses for survival (Figures 5A–5C) of placebo and drug-treated mice for each of the three trials demonstrated that CT53518 prolonged survival with p values of 0.001, 0.00005, and 0.0007 for trials 1, 2, and 3, respectively, using a log rank analysis. A combined Kaplan-Meier plot with the data from trials 1–3 is shown in Figure 5D.

Analysis of spleen weight and WBC counts from trial animals (Table 3) showed that in each of the three trials, the majority of placebo animals developed characteristic features of FLT3-ITD-induced myeloproliferative disease, while the majority of CT53518-treated mice did not. The median spleen weight was 563 mg for placebo animals, corresponding to a 5-fold increase in size compared to irradiated transplanted controls (100 mg). In contrast, CT53518-treated mice displayed only a slight increase in median spleen weight (189 mg). Similarly, the median WBC count for placebo animals was 23.0×10^6/ml compared to 4.3×10^6/ml for drug-treated animals. These results demonstrate that mice treated with CT53518 had a markedly reduced disease burden compared to untreated controls. It should be noted that in each trial, at least one CT53518-treated mouse had all of the manifestations of FLT3-ITD-induced MPD at study endpoint, which may reflect slight variability in disease burden or body weight in certain animals at onset of treatment.

For a subset of animals, WBC count was monitored at intervals throughout trial 2 by retroorbital sampling. Results from this analysis showed that total leukocyte counts from peripheral blood were all above normal range at the onset of therapy (12×10^6/ml–33×10^6/ml) and decreased to the normal range with therapy (Figure 6A) but not with placebo (Figure 6B), consistent with activity of CT53518 in reducing the disease burden. Comparison of WBC differentials for the mice from all three trials (Figure 6C) further demonstrated efficacy of CT53518 in treatment of FLT3-ITD-induced MPD. Whereas a wild-type untransplanted BALB/c mouse had approximately 69% lymphocytes and 23% neutrophils, the placebo mice with MPD had a reversal in these proportions to 18% lymphocytes and 74% neutrophils, reflecting a massive increase in myelopoiesis (Table 3). The relative proportions of eosinophils, monocytes, and basophils remained constant. In contrast, mice treated with CT53518 showed a normal total leukocyte count of 4.3×10^6/ml (Table 4), with a reversion to lymphocyte predominance in the differential (56% lymphocytes and 36% neutrophils) (Figure 6C).

At the endpoint for trial 3, a subset of drug-treated animals without physical evidence of disease were removed from drug therapy and monitored for subsequent signs of disease. After drug withdrawal, these animals developed classical FLT3-ITD myeloproliferative disease with a median latency of 45 days after cessation of drug (day 103) (Figure 6D; Kelly et al., 2002). At the time of sacrifice, the WBC counts and spleen weights of these animals (Table 3, trial 3) mirrored those for untreated FLT3-ITD trial mice. These data suggest that the treatment regimen carried out during this trial was not sufficient to eliminate all FLT3-ITD hematologic progenitor cells from the treated animals since removal of therapy results in the development of a MPD of similar latency and characteristics as that in untreated FLT3-ITD.

Histopathologic examination of the spleen from representative animals (Figure 6E) further supported the interpretation of a dramatic reduction in MPD in the drug-treated mice compared to placebo controls. The drug-treated animals showed a partial recovery of splenic architecture (Figure 6E, i), a reduction in myeloid hyperplasia, and a corresponding increase in the proportion of other hematopoietic lineages (Figure 6E, ii). These findings contrast with the effacement of splenic architecture observed in placebo mice due to marked expansion of red pulp comprised of maturing myeloid cells and scattered admixed megakaryocytes (Figure 6E, iii and iv). The spleen displayed characteristic features of a myeloproliferative disorder with marked hypercellularity and myeloid hyperplasia consisting predominantly of mature granulocytic elements (Figure 6E, iv).

The immunophenotype of single-cell suspensions from the spleens of five placebo and five CT53518-treated animals from trial 1 (Table 4) was examined using myeloid markers Gr-1 and

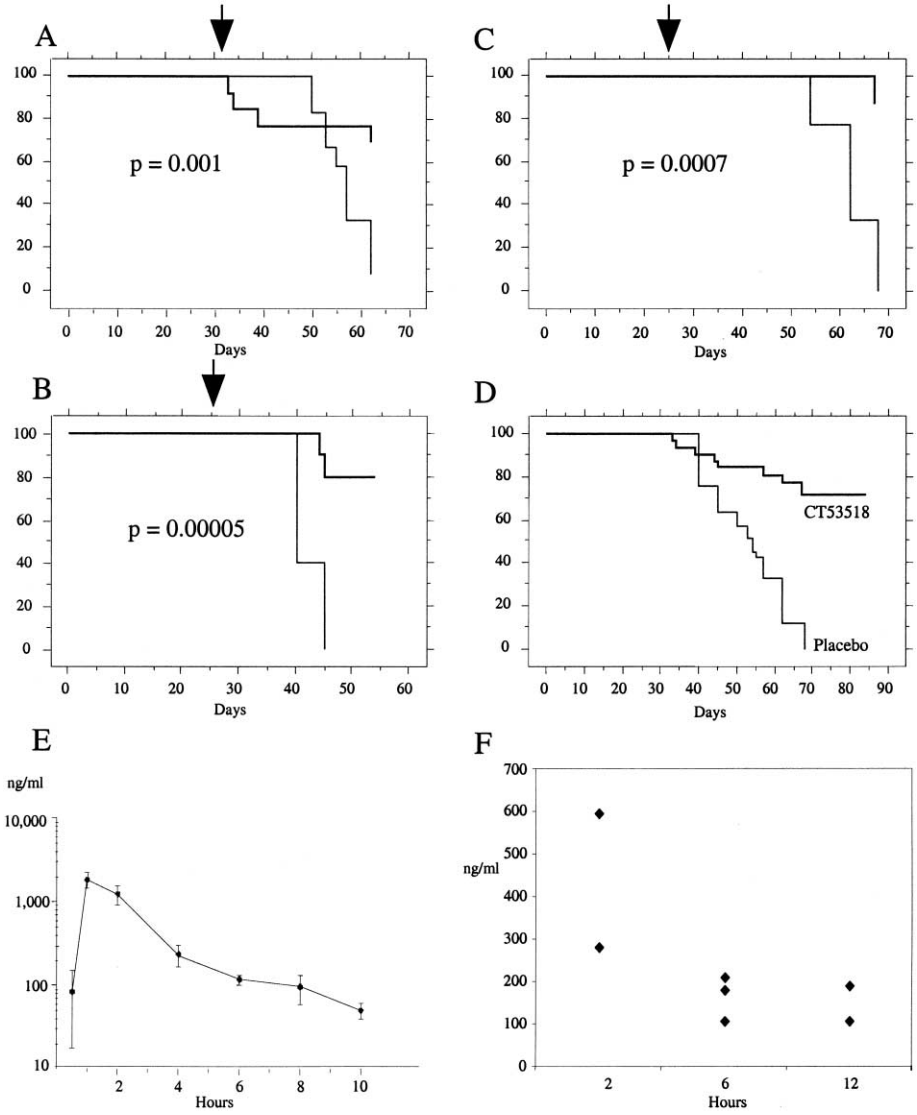

Figure 5. CT53518 increases survival in a murine BMT model of FLT3-ITD myeloproliferative disease

A–C: Mice transplanted with bone marrow transduced with Flt3-ITD/51 treated with placebo (n = 35) or with CT53518 at 120 mg/kg/day (n = 33). No mice were censored in this analysis. The percentage of surviving mice (*y* axis) is plotted with respect to time in days (*x* axis). The p value was obtained using the log rank test for binary outcome of dead or alive at the trial endpoint.
A: Trial 1, drug administered from day 32.
B: Trial 2, drug administered from day 25.
C: Trial 3, drug administered from day 25.
D: Combined data from trials 1–3.
E: Plasma concentration of CT53518 at different time intervals after a single oral dose of 60 mg/kg. Two or more mice at each time point were analyzed and the data is plotted as ng/ml.
F: Plasma concentration of CT53518 observed in drug-treated animals at trial endpoint. Plasma was collected from seven animals at 2 hr, 6 hr, and 12 hr after administration of the CT53518. The background measurement was set to zero in this graph and did not measure more than 5 ng.

Mac-1 to evaluate the proportion of myeloid cells present. These data showed that the placebo mice had an average of 60% myeloid cells compared to an average of 14% in the drug-treated group, which correspond closely to the peripheral blood differentials from these animals. Control irradiated and reconstituted mice typically display 10% Mac-1+ myeloid cells in the spleen. Southern analysis indicated that traces of the FLT3-ITD cDNA could be detected in the spleens of treated mice and the disease was still polyclonal (data not shown).

Discussion

An understanding of the genetic defects that are causally implicated in carcinogenesis has led to targeted therapy for the

Table 3. White blood cell counts (WBC, 10^6 per ml) and spleen weights (SW, mg) for placebo and CT53518-treated mice at trial endpoint

	Spleen Weight (mg)			CBC-WBC ($\times 10^6$/ml)		
	Placebo	CT53518	Off Drug	Placebo	CT53518	Off Drug
Mean	562	251	658	31.3	20.0	36.9
Median	563	189	595	23.0	4.3	33.8
Range	118–850	57–750	464–881	2.0–89.0	1.1–198	8.3–63.2
n	35	23	6	28	15	5

The mean and median values, range, and the number of animals (n) is listed. Placebo and CT53518 from all three trials are listed in the first two columns, and the third column reflects data from healthy mice taken off drug treatment at trial endpoint and sacrificed at 30 days later (trial 2) or at time of development of disease (trial 3).

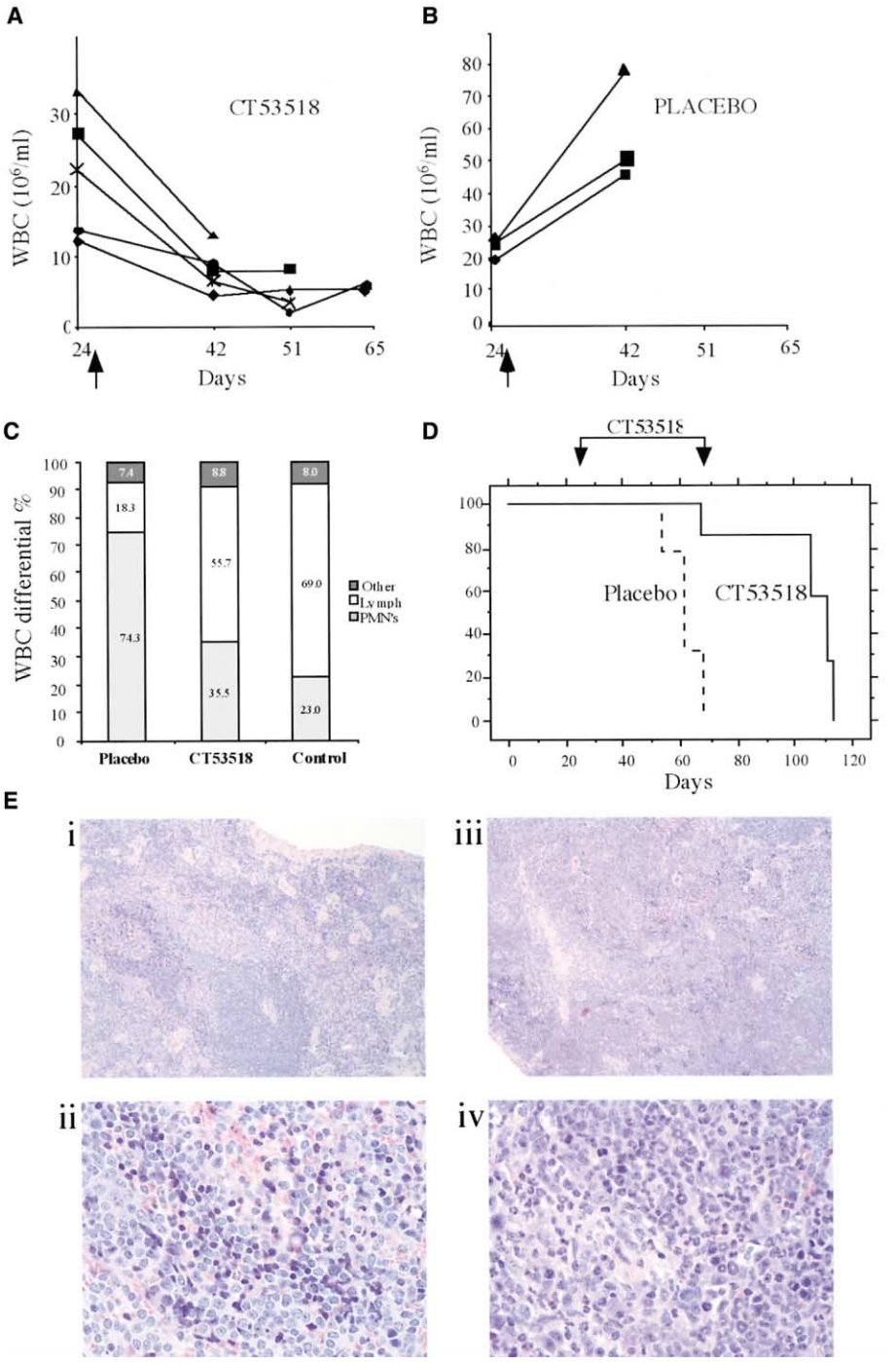

Figure 6. Response of white blood cells (WBC) and differential counts to CT53518 in peripheral blood

A and B: White blood cell counts from peripheral blood collected by retroorbital sampling, plotted as 10^6 white blood cells per ml over time. Onset of drug therapy (**A**) or placebo (**B**) is indicated by an arrowhead.

C: The average white blood cell differential counts from the peripheral blood of placebo (n = 13), drug-treated (n = 5), or wild-type BALB/c (n = 4) mice at trial endpoint are shown. The numbers are plotted to reflect the relative proportions of polymorphic neutrophils (PMN), lymphocytes (L), and other cells (Other), which includes monocytes, eosinophils, and basophils.

D: Kaplan-Meier plot of survival in off-drug animals. Mice transplanted with bone marrow transduced with Flt3-ITD treated with placebo (n = 9) or with CT53518 at 120 mg/kg/day (n = 6). Data is included from trial 3 only, with drug being administered from day 25 through day 65. The black arrow indicates the point at which drug therapy ceased. No mice were censored in this analysis. The percentage of surviving mice (*y* axis) is plotted with respect to time in days (*x* axis).

E: Histopathology of the spleen, sections stained with hematoxylin and eosin, for drug-treated 10× (**i**) and 50× (**ii**) or placebo mice 10× (**iii**) and 50× (**iv**). For description, see text.

treatment of CML and gastrointestinal stromal tumors (GIST) that harbor gain-of-function mutations in the c-Abl or c-Kit tyrosine kinases, respectively (Buchdunger et al., 2000; Carroll et al., 1997; Druker and Lydon, 2000; Druker et al., 2001a, 2001b; Joensuu et al., 2001; Mauro and Druker, 2001; Savage and Antman, 2002; Talpaz et al., 2002). A similar kinase inhibitor strategy may be effective for treatment of AML patients that have a FLT3 kinase gain-of-function mutations (Abu-Duhier et al., 2001; Kiyoi et al., 1999; Kottaridis et al., 2001; Nakao et al., 1996; Rombouts et al., 2000; Whitman et al., 2001; Yamamoto et al., 2001; Yokota et al., 1997). FLT3 is an attractive therapeutic target because of its high frequency in AML and because it confers a poor prognosis (Abu-Duhier et al., 2000; Kiyoi et al., 1999; Kottaridis et al., 2001). CT53518, a novel piperazinyl quanazoline, is a potent and selective antagonist of FLT3 and the closely related c-Kit and PDGFβR. CT53518 treatment inhibited FLT3-ITD autophosphorylation and factor-independent cell growth with an IC_{50} of 10–100 nM. CT53518 treatment of AML cell lines that harbor an endogenous FLT3-ITD induced apoptotic cell death, suggesting that FLT3 inhibitors might have

Table 4. Immunophenotype of cells from the spleen of placebo or drug-treated mice, documenting percentage of myeloid cells

	Mouse ID	Mac-1$^+$, Gr-1$^+$	Mac-1$^+$, Gr-1$^-$	Total Mac-1$^+$
Placebo	403	43.9	12.1	55.9
Placebo	404	43.3	11.6	54.8
Placebo	405	60.0	14.5	74.5
Placebo	406	57.8	11.0	68.8
Placebo	412	35.0	11.2	46.2
Average		47.9	12.1	60.0
CT53518	418	2.5	2.5	5.0
CT53518	419	31.8	8.7	40.4
CT53518	426	8.3	2.7	11.0
CT53518	427	4.4	1.9	6.3
CT53518	429	2.1	1.9	7.0
Average		10.4	3.5	14.0

Cells from five mice of each group were stained with APC-conjugated anti-Gr-1 and PE-conjugated Mac-1, or PE-Mac-1 alone. The cells were gated for live cells based on forward and side scatter profiles (M+M). The percentage of Mac-1, Gr-1 double-positive cells, the additional percentage of Mac-1 single-positive cells, and the total percentage of myeloid cells in each of the mice is listed.

efficacy in treatment of FLT3-ITD-positive AML blasts. The potential clinical application of CT53518 for the treatment of AML was further validated using mouse models of FLT3-ITD-mediated AML in which CT53518 treatment resulted in a significant decrease in disease progression and an increase in survival, confirming orally bioavailability and activity in vivo.

The AML cell line, MOLM 14, in which the FLT3-ITD mutation plays an essential role in cell proliferation and survival, provides a model system to characterize critical downstream effectors of FLT3 signal transduction in AML. Although studies on the mechanism of signal transduction by FLT3 are limited, signaling by the other type III RTKs, especially the PDGFR, has been studied extensively (Blume-Jensen and Hunter, 2001; Heldin and Westermark, 1999). PDGFR autophosphorylation creates docking sites for interaction with a number of signaling or adaptor proteins including the p85 subunit of PI-3 kinase, PLCγ, Src, STAT 5, Shc, Grb2, and Grb7 (Blume-Jensen and Hunter, 2001; Heldin and Westermark, 1999). The sites of tyrosine autophosphorylation for FLT3 have not been determined, but a phosphorylation-dependent interaction with Grb2, Src family members, PLCγ, and Shc has been reported. (Dosil et al., 1993; Marchetto et al., 1999; Zhang et al., 1999). A direct interaction with signaling molecules has not been reported for FLT3-ITDs, but their expression in IL-3-dependent hematopoietic cell lines results in the phosphorylation of STAT, Shc, Jak 2, Cbl, Erk, and Akt (Hayakawa et al., 2000; Lavagna-Sevenier et al., 1998; Mizuki et al., 2000; Rottapel et al., 1994; Tse et al., 2000). These studies indicate that FLT3-ITDs mediate sustained activation of the STAT, RAS/MAP kinase, and PI3 kinase pathways that are known to play a role in hematopoietic cell transformation (Benekli et al., 2002; Birkenkamp et al., 2001; Schuringa et al., 2000; Towatari et al., 1997; Rodriguez-Viciana et al., 1994; Testa and Bellacosa, 2001; Zhou et al., 2001).

Based on these considerations, we investigated the role of FLT3-ITD in RAS/MAP kinase pathway activation in Molm-14 cells by monitoring Erk2 phosphorylation. A high level of constitutive Erk2 phosphorylation was observed in Molm-14 and in FLT3-ITD-negative THP-1 cells. However, treatment with CT53518 only blocks Erk2 phosphorylation in FLT3-ITD-positive Molm-14 cells. Similarly, CT53518 selectively blocked Akt phosphorylation in FLT3-ITD-positive AML cells. This study indicates that in AML cell lines, FLT3-ITD may be the sole mechanism for constitutive activation of the RAS/MAP kinase and PI3/Akt kinase pathways.

In summary, we have developed CT53518, a potent and specific FLT3 kinase inhibitor for the treatment of FLT3-ITD-positive AML. This drug has been developed specifically for the purpose of treating AML associated with activating mutations in FLT3. CT53518 is well suited for these purposes based on preclinical studies in animals where it has high oral bioavailability, a long plasma half-life, a good safety profile with chronic administration, and efficacy in a mouse model of FLT3-ITD-mediated disease in primary hematopoietic cells. Further support for this strategy is provided by the observation that CT53518 induces apoptosis of FLT3-ITD-positive AML cells, a result similar to that observed when BCR/ABL-positive leukemia cells are treated with STI571 (Beran et al., 1998, Fang et al., 2000; Oetzel et al., 2000). It is thus quite possible that CT53518, or other classes of FLT3 inhibitors, will have clinical utility in treatment of AML. The ultimate success of this therapeutic strategy now awaits the outcome of clinical trials that are underway to evaluate the efficacy of CT53518 for the treatment of AML. However, based on recent reports of efficacy of STI571 in treatment of CML blast crisis and the comparable effects of CT53518 in this preclinical analysis, CT53518 shows great promise for treating this poor prognostic group of AML patients.

Experimental procedures

Kinase assays for CT53518 specificity analysis

All receptor tyrosine kinase assays were cell based and have been described previously (Yu et al., 2001) except for the insulin receptor (InsR) kinase assay, which was an enzyme-based assay measuring phosphorylation of the histone H2b substrate (GIBCO-BRL, Gaithursburg, MD). Briefly, 500 ng of purified recombinant InsR (Calbiochem, San Diego, CA) was incubated with a 20 μl reaction mixture containing 25 mM HEPES (pH 8), 25 mM $MgCl_2$, 25 mM β-glycerophosphate, 2 mM DTT, 100 μM Na_3VO_4, 10 μM ATP, 5 μCi of [γ-^{33}P]ATP, and 5 μg of histone H2b in the presence or absence of 30 μM CT53518 at 30°C for 30 min. Samples were subjected to SDS-PAGE, and substrate phosphorylation was detected by autoradiography.

All nonreceptor tyrosine kinases, serine/threonine kinases, MAP kinases, and MAPK kinases assays were enzyme-based assays and were described previously (Yu et al., 2001) except that of the Abl kinase assay, for which phosphorylation of a specific peptide-EAIYAAPFAKKK substrate was used (Dorsey et al., 2000). Abl kinase reaction was performed by incubating 2 ng of purified bacterially expressed Abl tyrosine kinase (Calbiochem) with 50 μl of reaction mixture containing 25 mM HEPES (pH 8), 25 mM $MgCl_2$, 2

mM DTT, 10 μM ATP, 5 μCi of [γ-^{33}P]ATP, and 100 μM peptide substrate at 30°C for 10 min in the presence of various concentrations of CT53518 (0.01–30 μM), and the reaction was terminated by the addition of 50 μl of 1.5% ice-cold phosphoric acid. The quenched assay solution was transferred to a phosphocellulose membrane microplate (Millipore Corporation, Bedford, MA), which was subsequently washed and counted on a scintillation counter as described (Yu et al., 2001).

Cell culture and growth curves

Ba/F3 cells were maintained in RPMI, 10% FCS, and IL-3 (0.5 ng/ml, R&D Systems, Minneapolis, MN). Retroviral stocks were generated using MSCV constructs FLT3-ITD (Kelly et al., 2002), TEL/TRKc (Liu et al., 2000), TEL/PDGFβR (Tomasson et al., 1999), and BCR/ABL (Daley et al., 1990) as described previously (Kelly et al., 2002; Schwaller et al., 1998). Retrovirally transduced Ba/F3 cells were cultured for 48 hr and selected with G418 for 14 days and cultured in media without IL-3 to confirm factor-independent growth.

Molm-13 and Molm-14 cell lines of AML-M5a class were obtained from Fujisaki Cell Center (Okayama, Japan) and were cultured in RPMI 1640 supplemented with 10% FBS. AML cell lines HL60 (AML-M3) and AML193 (AML-M5), KG-1, KG-1a, THP-1, and ALL cell line RS4;11 were purchased from ATCC (Bethesda, MD) and were cultured according to supplier's specifications. Cells (initial count of 0.3×10^5–1.0×10^5) were washed three times in RPMI 1640 medium and plated in 1 ml of complete growth media (without IL-3 for the Ba/F3 cells) in the presence of increasing concentrations of CT53518 (0.004–30 μM). Cells were grown for 3–7 days in tissue culture, and viable cells, determined by Trypan blue dye exclusion, were counted.

Immunoprecipitation and immunoblot analyses

Cells were incubated with CT53518 (0.003–10 μM) at room temperature for 30 min prior to ligand stimulation (37°C, 10 min) followed by cell lysis as described (Yu et al., 2001). Lysates were subjected to immunoprecipitation and immunoblot analyses with the indicated antibodies that include anti-FLT3 polyclonal, anti-phosphotyrosine monoclonal (both from Santa Cruz Biotechnology, Santa Cruz, CA), anti-phospho-Erk2 polyclonal, and anti-phospho-Akt1 polyclonal (both from Cell Signaling Technology, Beverly, MA) antibodies.

Apoptosis analysis

Fluorescein isothiocyanate (FITC)-conjugated annexin V (Becton Dickson Biosciences, San Diego, CA) binding to phospholipid phosphatidylserine was used to evaluate CT53518-induced cell apoptosis using flow cytometry techniques. AML cells were plated at 2.5×10^5 per well in 24-well plates in growth medium with 1 μM of CT53518. At daily intervals, cells were harvested, washed, and resuspended in 100 μl binding buffer containing 10 mM HEPES (pH 7.4), 140 mM NaCl, and 2.5 mM $CaCl_2$. Annexin V-FITC (100 ng) and propidium iodide (250 ng) were added to the cell suspension followed by incubation at room temperature for 15 min. Flow cytometry was performed immediately after staining on a FACSort flow cytometer (Becton Dickson) with excitation at 488 nm. Fluorescence of annexin V-FITC and DNA propidium iodide staining were measured at 515 nm and 585 nm, respectively.

Drug preparation and administration

CT53518 was prepared as a powder and stored at 4°C and resuspended in a 0.5% methylcellulose (MC) in water solution prior to use. Dosing of drug (40–120 mg/kg/day) or placebo (MC only) was performed every 12 hr by gavage (100 μl) using 22-gauge needles (Hornbecks). Plasma concentrations of the drug were calculated by mass spectrometry using 50 μl of plasma.

Ba/F3 FLT3-ITD nude mice xenograft leukemia model

Athymic nude mice ($n = 10$ for each CT53518-treated or vehicle control group) were each injected via marginal tail vein with 1×10^6 Ba/F3 cells expressing W51 FLT3-ITD mutant. Mice were not dosed in the first week to allow FLT3-ITD-expressing cells to initiate disease. In the second study, an extra group of mice were orally dosed BID at 20 mg/kg of CT53518. Dosing continued until day 42 or day 57 in the two studies. For statistical analysis, a log-rank test was used to compare the difference between vehicle- and CT53518-treated groups. Differences were statistically significant at $p \leq 0.05$.

Transplant model

Bone marrow transplantation assays with 1×10^6–3×10^6 cells were carried out as described previously (Schwaller et al., 1998; Liu et al., 2000; Kelly et al., 2002).

Any animals with splenomegaly (spleen boundary detectable at the dorsal midline) or that were moribund were sacrificed and analyzed for signs of MPD.

Peripheral blood was collected from the retroorbital cavity using a heparinized glass capillary. Blood smears were stained with Wright and Giemsa. Manual and automated (ADIVA 120 Hematology system, Bayer) total and differential blood cell counts were performed. Histopathologic exam of relevant organs (spleen, liver, heart, lungs, intestine, hindlimb bones, and kidneys) and preparation of single-cell suspensions from spleen and bone marrow for flow cytometry was performed as described (Schwaller et al., 1998; Liu et al., 2000; Kelly et al., 2002). In each trial, mice were dosed with either drug or placebo. Assuming that 20% of drug-treated animals and 80% of untreated animals would develop an MPD, we designed our trial to have 80% power to detect this difference at the 0.05% significance level using 11 mice. In comparing the survival time of the mice, all times are measured from the day of BMT, and the log rank test is used to attach a significance level to the difference in the survival curves. Mice alive at the end of the study or that were sacrificed in an apparently healthy condition at the end of the study were considered censored in this analysis.

Acknowledgments

We gratefully acknowledge valuable discussions with members of Millenium Pharmaceuticals and the Gilliland lab, and the administrative assistance of Lindsay Seaton. This work was supported in part the by Leukemia and Lymphoma Society and the MarJo Tournament (L.M.K. and D.G.G.) and National Institutes of Health grants CA66996 and DK50654. D.G.G. is an investigator and L.M.K. is an associate of the Howard Hughes Medical Institute.

Received: April 22, 2002
Revised: May 29, 2002
Published online: May 31, 2002

References

Abu-Duhier, F.M., Goodeve, A.C., Wilson, G.A., Gari, M.A., Peake, I.R., Rees, D.C., Vandenberghe, E.A., Winship, P.R., and Reilly, J.T. (2000). FLT3 internal tandem duplication mutations in adult acute myeloid leukaemia define a high-risk group. Br. J. Haematol. *111*, 190–195.

Abu-Duhier, F.M., Goodeve, A.C., Wilson, G.A., Care, R.S., Peake, I.R., and Reilly, J.T. (2001). Identification of novel FLT-3 Asp835 mutations in adult acute myeloid leukaemia. Br. J. Haematol. *113*, 983–988.

Benekli, M., Xia, Z., Donohue, K.A., Ford, L.A., Pixley, L.A., Baer, M.R., Baumann, H., and Wetzler, M. (2002). Constitutive activity of signal transducer and activator of transcription 3 protein in acute myeloid leukemia blasts is associated with short disease-free survival. Blood *99*, 252–257.

Beran, M., Cao, X., Estrov, Z., Jeha, S., Jin, G., O'Brien, S., Talpaz, M., Arlinghaus, R.B., Lydon, N.B., and Kantarjian, H. (1998). Selective inhibition of cell proliferation and BCR-ABL phosphorylation in acute lymphoblastic leukemia cells expressing Mr 190,000 BCR-ABL protein by a tyrosine kinase inhibitor (CGP-57148). Clin. Cancer Res. *4*, 1661–1672.

Birkenkamp, K.U., Geugien, M., Lemmink, H.H., Kruijer, W., and Vellenga, E. (2001). Regulation of constitutive STAT5 phosphorylation in acute myeloid leukemia blasts. Leukemia *15*, 1923–1931.

Blume-Jensen, P., and Hunter, T. (2001). Oncogenic kinase signalling. Nature *411*, 355–365.

Buchdunger, E., Cioffi, C.L., Law, N., Stover, D., Ohno-Jones, S., Druker, B.J., and Lydon, N.B. (2000). Abl protein-tyrosine kinase inhibitor STI571 inhibits in vitro signal transduction mediated by c-kit and platelet-derived growth factor receptors. J. Pharmacol. Exp. Ther. *295*, 139–145.

Carroll, M., Ohno-Jones, S., Tamura, S., Buchdunger, E., Zimmermann, J., Lydon, N.B., Gilliland, D.G., and Druker, B.J. (1997). CGP 57148, a tyrosine kinase inhibitor, inhibits the growth of cells expressing BCR-ABL, TEL-ABL, and TEL-PDGFR fusion proteins. Blood *90*, 4947–4952.

Daley, G.Q., Van Etten, R.A., and Baltimore, D. (1990). Induction of chronic myelogenous leukemia in mice by the P210$^{bcr/abl}$ gene of the Philadelphia chromosome. Science *247*, 824–830.

Dorsey, J.F., Jove, R., Kraker, A.J., and Wu, J. (2000). The pyrido[2,3-d]pyrimidine derivative PD180970 inhibits p210Bcr-Abl tyrosine kinase and induces apoptosis of K562 leukemic cells. Cancer Res. *60*, 3127–3131.

Dosil, M., Wang, S., and Lemischka, I.R. (1993). Mitogenic signalling and substrate specificity of the Flk2/Flt3 receptor tyrosine kinase in fibroblasts and interleukin 3-dependent hematopoietic cells. Mol. Cell. Biol. *13*, 6572–6585.

Druker, B.J., and Lydon, N.B. (2000). Lessons learned from the development of an abl tyrosine kinase inhibitor for chronic myelogenous leukemia. J. Clin. Invest. *105*, 3–7.

Druker, B.J., Tamura, S., Buchdunger, E., Ohno, S., Segal, G.M., Fanning, S., Zimmermann, J., and Lydon, N.B. (1996). Effects of a selective inhibitor of the Abl tyrosine kinase on the growth of Bcr-Abl positive cells. Nat. Med. *2*, 561–566.

Druker, B.J., Sawyers, C.L., Kantarjian, H., Resta, D.J., Reese, S.F., Ford, J.M., Capdeville, R., and Talpaz, M. (2001a). Activity of a specific inhibitor of the BCR-ABL tyrosine kinase in the blast crisis of chronic myeloid leukemia and acute lymphoblastic leukemia with the Philadelphia chromosome. N. Engl. J. Med. *344*, 1038–1042.

Druker, B.J., Talpaz, M., Resta, D.J., Peng, B., Buchdunger, E., Ford, J.M., Lydon, N.B., Kantarjian, H., Capdeville, R., Ohno-Jones, S., and Sawyers, C.L. (2001b). Efficacy and safety of a specific inhibitor of the BCR-ABL tyrosine kinase in chronic myeloid leukemia. N. Engl. J. Med. *344*, 1031–1037.

Fang, G., Kim, C.N., Perkins, C.L., Ramadevi, N., Winton, E., Wittmann, S., and Bhalla, K.N. (2000). CGP57148B (STI-571) induces differentiation and apoptosis and sensitizes Bcr-Abl-positive human leukemia cells to apoptosis due to antileukemic drugs. Blood *96*, 2246–2253.

Hayakawa, F., Towatari, M., Kiyoi, H., Tanimoto, M., Kitamura, T., Saito, H., and Naoe, T. (2000). Tandem-duplicated Flt3 constitutively activates STAT5 and MAP kinase and introduces autonomous cell growth in IL-3-dependent cell lines. Oncogene *19*, 624–631.

Heldin, C.H., and Westermark, B. (1999). Mechanism of action and in vivo role of platelet-derived growth factor. Physiol. Rev. *79*, 1283–1316.

Iida, M., Towatari, M., Nakao, A., Iida, H., Kiyoi, H., Nakano, Y., Tanimoto, M., Saito, H., and Naoe, T. (1999). Lack of constitutive activation of MAP kinase pathway in human acute myeloid leukemia cells with N-Ras mutation. Leukemia *13*, 585–589.

Joensuu, H., Roberts, P.J., Sarlomo-Rikala, M., Andersson, L.C., Tervahartiala, P., Tuveson, D., Silberman, S., Capdeville, R., Dimitrijevic, S., Druker, B., and Demetri, G.D. (2001). Effect of the tyrosine kinase inhibitor STI571 in a patient with a metastatic gastrointestinal stromal tumor. N. Engl. J. Med. *344*, 1052–1056.

Kelly, L.M., Liu, Q., Kutok, J.L., Williams, I.R., Boulton, C.L., and Gilliland, D.G. (2002). FLT3 internal tandem duplication mutations associated with human acute myeloid leukemias induce myeloproliferative disease in a murine bone marrow transplant model. Blood *99*, 310–318.

Kiyoi, H., Naoe, T., Nakano, Y., Yokota, S., Minami, S., Miyawaki, S., Asou, N., Kuriyama, K., Jinnai, I., Shimazaki, C., et al. (1999). Prognostic implication of FLT3 and N-RAS gene mutations in acute myeloid leukemia. Blood *93*, 3074–3080.

Kottaridis, P.D., Gale, R.E., Frew, M.E., Harrison, G., Langabeer, S.E., Belton, A.A., Walker, H., Wheatley, K., Bowen, D.T., Burnett, A.K., et al. (2001). The presence of a FLT3 internal tandem duplication in patients with acute myeloid leukemia (AML) adds important prognostic information to cytogenetic risk group and response to the first cycle of chemotherapy: analysis of 854 patients from the United Kingdom Medical Research Council AML 10 and 12 trials. Blood *98*, 1752–1759.

Lavagna-Sevenier, C., Marchetto, S., Birnbaum, D., and Rosnet, O. (1998). The CBL-related protein CBLB participates in FLT3 and interleukin-7 receptor signal transduction in pro-B cells. J. Biol. Chem. *273*, 14962–14967.

Liu, Q., Schwaller, J., Kutok, J., Cain, D., Aster, J.C., Williams, I.R., and Gilliland, D.G. (2000). Signal transduction and transforming properties of the TEL-TRKC fusions associated with t(12;15)(p13;q25) in congenital fibrosarcoma and acute myelogenous leukemia. EMBO J. *19*, 1827–1838.

Lowenberg, B., Downing, J.R., and Burnett, A. (1999). Acute myeloid leukemia. N. Engl. J. Med. *341*, 1051–1062.

Marchetto, S., Fournier, E., Beslu, N., Aurran-Schleinitz, T., Dubreuil, P., Borg, J.P., Birnbaum, D., and Rosnet, O. (1999). SHC and SHIP phosphorylation and interaction in response to activation of the FLT3 receptor. Leukemia *13*, 1374–1382.

Matsuo, Y., MacLeod, R.A., Uphoff, C.C., Drexler, H.G., Nishizaki, C., Katayama, Y., Kimura, G., Fujii, N., Omoto, E., Harada, M., and Orita, K. (1997). Two acute monocytic leukemia (AML-M5a) cell lines (MOLM-13 and MOLM-14) with interclonal phenotypic heterogeneity showing MLL-AF9 fusion resulting from an occult chromosome insertion, ins(11;9)(q23;p22p23). Leukemia *11*, 1469–1477.

Mauro, M.J., and Druker, B.J. (2001). STI571: targeting BCR-ABL as therapy for CML. Oncologist *6*, 233–238.

Mizuki, M., Fenski, R., Halfter, H., Matsumura, I., Schmidt, R., Muller, C., Gruning, W., Kratz-Albers, K., Serve, S., Steur, C., et al. (2000). Flt3 mutations from patients with acute myeloid leukemia induce transformation of 32D cells mediated by the Ras and STAT5 pathways. Blood *96*, 3907–3914.

Nakao, M., Yokota, S., Iwai, T., Kaneko, H., Horiike, S., Kashima, K., Sonoda, Y., Fujimoto, T., and Misawa, S. (1996). Internal tandem duplication of the flt3 gene found in acute myeloid leukemia. Leukemia *10*, 1911–1918.

Oetzel, C., Jonuleit, T., Gotz, A., van der Kuip, H., Michels, H., Duyster, J., Hallek, M., and Aulitzky, W.E. (2000). The tyrosine kinase inhibitor CGP 57148 (ST1 571) induces apoptosis in BCR-ABL-positive cells by down-regulating BCL-X. Clin. Cancer Res. *6*, 1958–1968.

Rodriguez-Viciana, P., Warne, P.H., Dhand, R., Vanhaesebroeck, B., Gout, I., Fry, M.J., Waterfield, M.D., and Downward, J. (1994). Phosphatidylinositol-3-OH kinase as a direct target of Ras. Nature *370*, 527–532.

Rombouts, W.J., Blokland, I., Lowenberg, B., and Ploemacher, R.E. (2000). Biological characteristics and prognosis of adult acute myeloid leukemia with internal tandem duplications in the Flt3 gene. Leukemia *14*, 675–683.

Rottapel, R., Turck, C.W., Casteran, N., Liu, X., Birnbaum, D., Pawson, T., and Dubreuil, P. (1994). Substrate specificities and identification of a putative binding site for PI3K in the carboxy tail of the murine Flt3 receptor tyrosine kinase. Oncogene *9*, 1755–1765.

Savage, D.G., and Antman, K.H. (2002). Imatinib mesylate—a new oral targeted therapy. N. Engl. J. Med. *346*, 683–693.

Schuringa, J.J., Wierenga, A.T., Kruijer, W., and Vellenga, E. (2000). Constitutive Stat3, Tyr705, and Ser727 phosphorylation in acute myeloid leukemia cells caused by the autocrine secretion of interleukin-6. Blood *95*, 3765–3770.

Schwaller, J., Frantsve, J., Tomasson, M., Aster, J., Williams, I., Van Rompey, L., Marynen, P., Van Etten, R., Ilaria, R., and Gilliland, D.G. (1998). Transformation of hematopoietic cell lines to growth-factor independence and induction of a fatal myeloid and lymphoproliferative disease in mice by retrovirally transduced TEL/JAK2 fusion gene. EMBO J. *17*, 5321–5333.

Stephens, L., Anderson, K., Stokoe, D., Erdjument-Bromage, H., Painter, G.F., Holmes, A.B., Gaffney, P.R., Reese, C.B., McCormick, F., Tempst, P., et al. (1998). Protein kinase B kinases that mediate phosphatidylinositol 3,4,5-trisphosphate-dependent activation of protein kinase B. Science *279*, 710–714.

Stirewalt, D.L., Kopecky, K.J., Meshinchi, S., Appelbaum, F.R., Slovak, M.L., Willman, C.L., and Radich, J.P. (2001). FLT3, RAS, and TP53 mutations in elderly patients with acute myeloid leukemia. Blood *97*, 3589–3595.

Stokoe, D., Stephens, L.R., Copeland, T., Gaffney, P.R., Reese, C.B., Painter, G.F., Holmes, A.B., McCormick, F., and Hawkins, P.T. (1997). Dual role of

phosphatidylinositol-3,4,5-trisphosphate in the activation of protein kinase B. Science *277*, 567–570.

Talpaz, M., Silver, R.T., Druker, B.J., Goldman, J.M., Gambacorti-Passerini, C., Guilhot, F., Schiffer, C.A., Fischer, T., Deininger, M.W., Lennard, A.L., et al. (2002). Imatinib induces durable hematologic and cytogenetic responses in patients with accelerated phase chronic myeloid leukemia: results of a phase 2 study. Blood *99*, 1928–1937.

Testa, J.R., and Bellacosa, A. (2001). AKT plays a central role in tumorigenesis. Proc. Natl. Acad. Sci. USA *98*, 10983–10985.

Tomasson, M.H., Williams, I.R., Hasserjian, R., Udomsakdi, C., McGrath, S.M., Schwaller, J., Druker, B., and Gilliland, D.G. (1999). TEL/PDGFβR induces hematologic malignancy in mice that responds to the tyrosine kinase inhibitor CGP57148. Blood *93*, 1707–1714.

Towatari, M., Iida, H., Tanimoto, M., Iwata, H., Hamaguchi, M., and Saito, H. (1997). Constitutive activation of mitogen-activated protein kinase pathway in acute leukemia cells. Leukemia *11*, 479–484.

Tse, K.F., Mukherjee, G., and Small, D. (2000). Constitutive activation of FLT3 stimulates multiple intracellular signal transducers and results in transformation. Leukemia *14*, 1766–1776.

Whitman, S.P., Archer, K.J., Feng, L., Baldus, C., Becknell, B., Carlson, B.D., Carroll, A.J., Mrozek, K., Vardiman, J.W., George, S.L., et al. (2001). Absence of the wild-type allele predicts poor prognosis in adult de novo acute myeloid leukemia with normal cytogenetics and the internal tandem duplication of FLT3: a cancer and leukemia group B study. Cancer Res. *61*, 7233–7239.

Yamamoto, Y., Kiyoi, H., Nakano, Y., Suzuki, R., Kodera, Y., Miyawaki, S., Asou, N., Kuriyama, K., Yagasaki, F., Shimazaki, C., et al. (2001). Activating mutation of D835 within the activation loop of FLT3 in human hematologic malignancies. Blood *97*, 2434–2439.

Yokota, S., Kiyoi, H., Nakao, M., Iwai, T., Misawa, S., Okuda, T., Sonoda, Y., Abe, T., Kahsima, K., Matsuo, Y., and Naoe, T. (1997). Internal tandem duplication of the FLT3 gene is preferentially seen in acute myeloid leukemia and myelodysplastic syndrome among various hematological malignancies. A study on a large series of patients and cell lines. Leukemia *11*, 1605–1609.

Yu, J.C., Lokker, N.A., Hollenbach, S., Apatira, M., Li, J., Betz, A., Sedlock, D., Oda, S., Nomoto, Y., Matsuno, K., et al. (2001). Efficacy of the novel selective platelet-derived growth factor receptor antagonist CT52923 on cellular proliferation, migration, and suppression of neointima following vascular injury. J. Pharmacol. Exp. Ther. *298*, 1172–1178.

Zhang, S., Mantel, C., and Broxmeyer, H. (1999). Flt3 signaling involves tyrosyl-phosphorylation of SHP-2 and SHIP and their association with Grb2 and Shc in Baf3/Flt3 cells. J. Leukoc. Biol. *65*, 372–380.

Zhou, B.P., Liao, Y., Xia, W., Zou, Y., Spohn, B., and Hung, M.C. (2001). HER-2/neu induces p53 ubiquitination via Akt-mediated MDM2 phosphorylation. Nat. Cell Biol. *3*, 973–982.